Supporting information

A mechanically strong and self-adhesive all-solid-state ionic conductor based on the double-network strategy

Yue Han,‡[a] Kai Zhao,‡[b] Guangxue Chen*[a], Ren'ai Li,[c] Chuhan Zhou,[a] Ziyu Hua,[a] Huawei Duan[d] and Minghui He*[a]

[a] State Key Laboratory of Pulp and Paper Engineering, School of Light Industry and Engineering, South China University of Technology, Guangzhou 510640, China.

[b] Department of Chemical Engineering, Tsinghua University, Beijing, 100084, China.

[c] Jiangsu Co-innovation Center for Efficient Processing and Utilization of Forest Resources, Jiangsu Provincial Key Lab Pulp & Paper Science and Technology, Nanjing Forestry University, Nanjing 210037, China.

[d] Department of Science Research, Great Bay University, Dongguan 523000, China.

‡ These authors contributed equally to this work.

* Corresponding author's E-mail: heminghui@scut.edu.cn; chengx@scut.edu.cn

Experimental Section

Materials.

Choline dihydrogen citrate (CDC, 98%, Shanghai Maclean Biochemical Co., Ltd.), acrylic acid (AA, >99%, Macklin), lignin (Dealkaline) (DL, Shanghai Aladdin Reagent), diphenyl(2,4,6-trimethylbenzoyl) phosphine oxide (TPO, 97%, Shanghai Aladdin Reagent) were used as receiving materials.

Synthesis of lignin-PDES mixture.

AA was dried on 4Å molecular sieves before use. First, CDC and AA were mixed in a molar ratio of 1:2. Then, the mixture was heated and stirred at 90°C for about 30 min in a closed flask, and the resulting clear and transparent solution was placed in a vacuum desiccator with silica gel for use. Then, 0-1wt.% of lignin (dealkaline) was introduced and the mixture was heated and stirred for 30 min to form a transparent, precipitation-free lignin-PDES mixture. The prepared lignin-PDES mixture were then stored in a vacuum desiccator along with silica gel until further use.

Synthesis of ADNICs.

ADNICs were synthesized by in situ polymerization of pre-cured solution by UV light. The photoinitiator (TPO) was introduced into the above clear solution (the amount of photoinitiator added was 1 wt.% of the PDES monomers mass). Continue to stir in a 90°C oil bath for 10min until the mixture is uniform, pour it into a 1mm thick silica gel model sandwiched between two glass plates, and irradiate it with a 20mW.cm^{-2} UV light source for 2 min to prepare an ionic conductor. They are denoted as ADNIC-x (x is the percentage of lignin in the total mass, and the ionic conductors used in the thin film characterization are all ADNIC-0.5). The shape and thickness of the prepared polymer can be freely adjusted according to the silica gel sheet. Unless otherwise specified, the thickness of the films used in this experiment is all 1 mm.

Characterizations.

Fourier transform infrared spectra (FTIR) were recorded on a Bruker Vertex 33 spectrometer. Test 1H NMR spectrum (400 MHz) using Bruker spectrometer AVANCE III HD 400. Differential scanning calorimetry (DSC) was performed using a 214 polyma-NETZSCH tester. The ADNIC films were placed in an aluminum tray and heated from -80˚C to 80˚C at 10˚C min^{-1} under a nitrogen atmosphere. Optical transmittance was measured using an Agilent cary60 UV-Vis spectrophotometer with a wavelength range of 200–800 nm. The relationship between the mass and temperature of the ionic conductor was studied using a TG209F3 thermogravimetric tester. Take 8-10 mg of the dried sample and place it in a thermogravimetric tester (TG209F3), set the nitrogen flow rate to 10 ml min^{-1}, and conduct the test at a heating rate of 20 ˚C min^{-1} in the temperature range of 40-700 °C. Microstructure and phase diagrams of ADNICs were taken using atomic force microscopy (AFM). Optical, electrical, and mechanical demonstration images were taken with a Canon 760D camera.

The ionic conductivity was measured using electrochemical impedance spectroscopy (EIS) at frequencies from 1 to 100 Hz in an electrochemical workstation (CHI600E). After the sample is cut into a size of 10×10×1mm, it is sandwiched between two copper plates. The calculation formula is: $\sigma=L/(R\times A)$, where L represents the thickness of the film, R represents the resistance, and A represents the area of the two copper plates in contact. The parameter is set as follows: 200mA current range, $10^{-1}\sim10^{6}$Hz.

Tensile tests were performed using tensile machine (INSTRON 5565, 100N load cell). The test conditions were as follows: rectangular samples of 50mm×20mm×1mm were stretched at the speed of 10 mm min^{-1},25 mm min^{-1} and 50 mm min^{-1}.

Lap shear tests were performed on a tensile machine (INSTRON 5565, 100 N load cell) with a layer of ADNIC film (10mm×10mm) sandwiched between two substrates (20mm×50mm) at a speed of 10 mm min^{-1}.

For the 90º peel test, the ADNIC films were fixed on the tester (INSTRON 5565, 100N load cell) so that the material was in close contact with the sample, and the length, width, and height of the contact section is 50mm×20 mm×1mm, and the peel

test is performed at a speed of 10 mm min^{-1}.

Self-healing experiments were performed by using a razor blade to completely cut the samples in half and then making them come into contact with each other. The healed samples were tested after being left at room temperature at various times. Self-healing photographs were taken using a research-grade orthogonal microscope (OLYMPUS BX51, Japan)

Digital source meter (Keithley DMM7510) was used to detect the electrical response of ADNICs self-adhesive strain sensors. $\Delta R/R_0$ is defined as the relative resistance change during deformation, where R_0 is the initial value when undeformed and R is the corresponding resistance at a certain level of deformation.

Molecular Dynamic Simulation

Lignin, PAA (n=3), Choline dihydrogen citrate(CDC) were performed geometry optimizations using density functional theory B3LYP/def-TZVP with DFT-D3 dispersion correction. Ambertools21[1] and ACPYPE[2] were used to construct the general AMBER force field 2(GAFF2) parameters[3], Multiwfn[4] was used to fit the restrained electrostatic potential (RESP) charge; Molecular dynamics (MD) simulation of PAA-CDC-lignin system was performed using GROMACS 2021.5 package.[5] Cubic box with initial dimensions of $8\times8\times8nm^3$ packed with components was constructed using packmol program,[6] and energy minimization was performed by using the steepest descent algorithm with a force tolerance of 500 kJ mol^{-1} nm^{-1}. In all three directions, periodic boundary conditions were imposed. Then the system was relaxed for 1 ns under NPT ensemble.

After completing the above steps, 50ns NPT MD simulation was performed. The pressure was maintained at 1 bar by the Berendsen barostat[7] in an isotropic manner and the temperature was controlled by the V-rescal thermostat.[8] In the first 20 ns, the system was annealed twice with 298 K-498 K-298 K, and the temperature was kept at 298K for the last 30 ns. The LINCS algorithm was performed to constrain the bond lengths of hydrogen atoms. Lennard-Jones interactions were calculated within a cutoff of 1.2 nm, and electrostatic interactions beyond 1.2 nm were treated with the particle-

mesh Ewald (PME) method with a grid spacing of 0.16 nm. UCSF ChimeraX[9] was used to visualize all results.
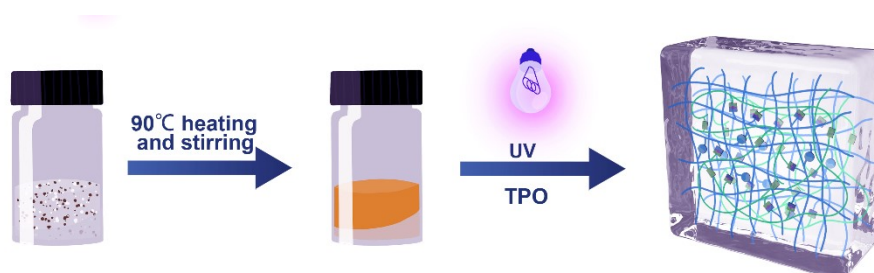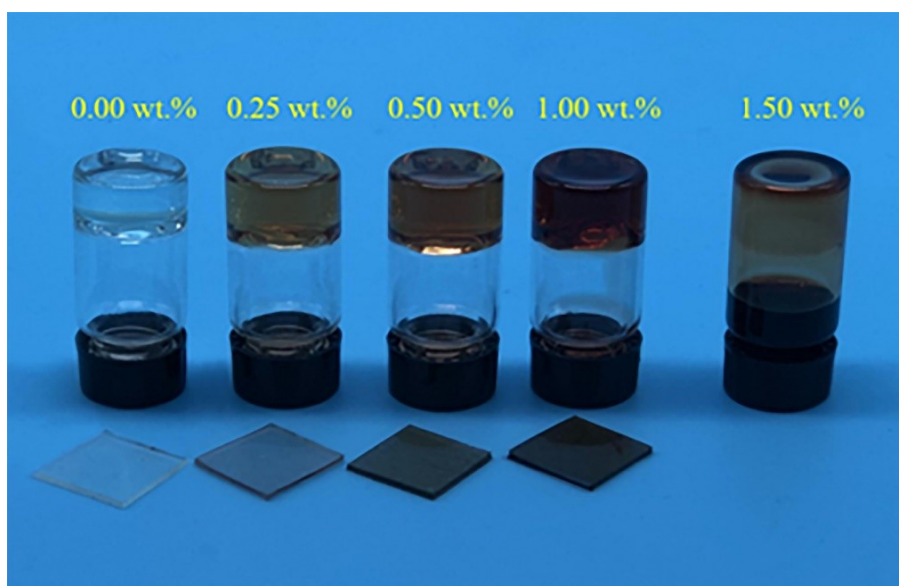

Fig. S1. Synthesis process of ADNICs.

Fig. S2. Digital photographs of ADNICs with different lignin contents after photopolymerization.

Table S1. Detailed composition of the various ADNICs.

PDES preparation	Sample (wt.%)	Color	Polymerization 2 minutes
	0	Colorless and transparent	Ionic conductor, rigid
CDC: AA=1:2	0.25	Yellow	Ionic conductor, rigid
(mole ratio)	0.5	Brown	Ionic conductor，Stretchable
	1	Dark Brown	Ionic conductor，Stretchable
☐	1.5	Brown-black	Liquids
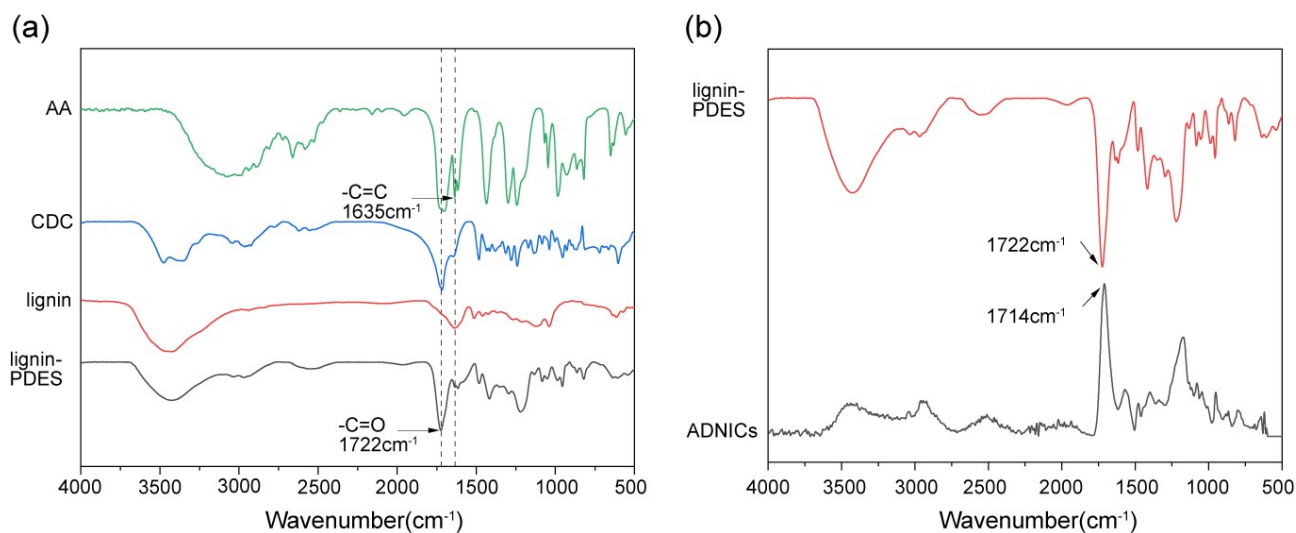
Fig. S3. (a)The FTIR curves of lignin-PDES mixture with AA, CDC and lignin. (b)The FTIR spectroscopy of lignin-PDES mixture and ADNICs generated by their polymerization.
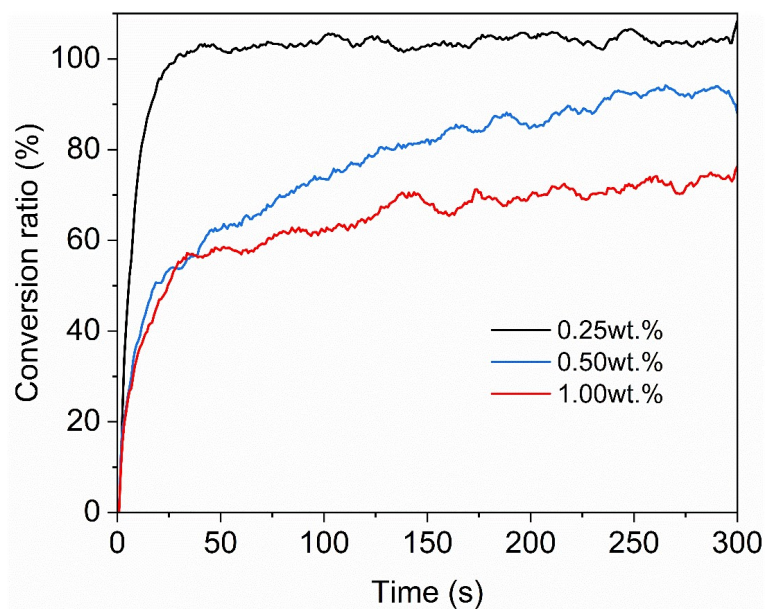

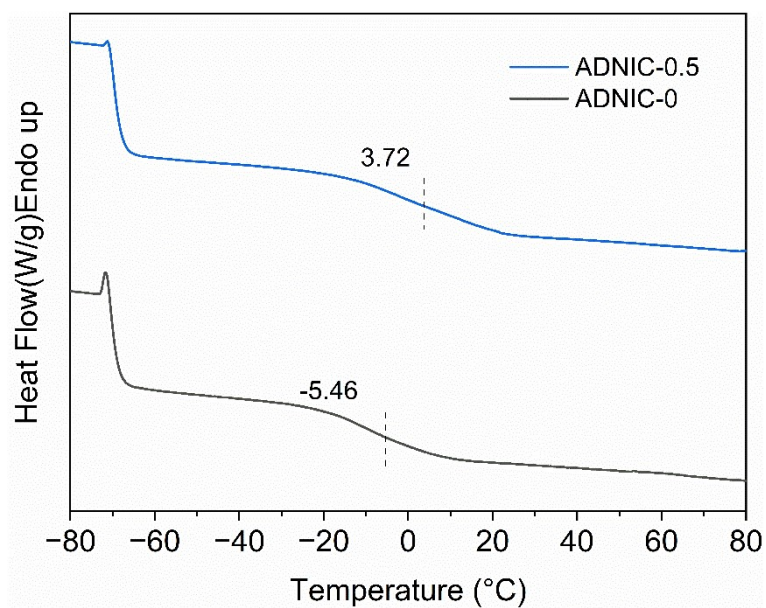**Fig. S4.** (a) -C=C double bond conversion of PDES monomer.

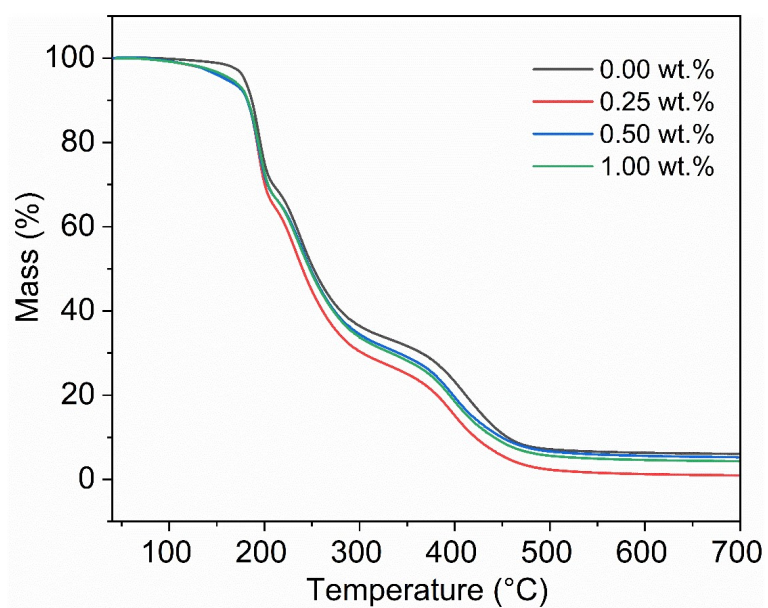**Fig. S5.** Differential scanning calorimetry (DSC) profiles of ADNIC-0 and ADNIC-0.5.

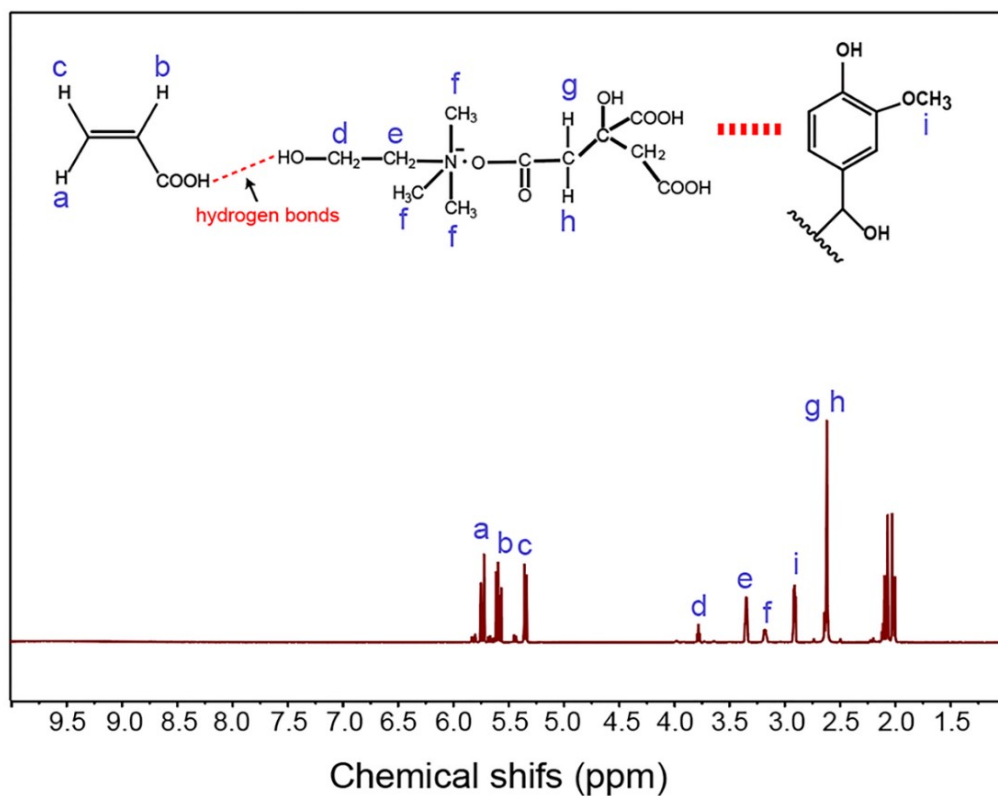**Fig. S6.** Thermogravimetric analysis of ADNICs with different lignin contents.

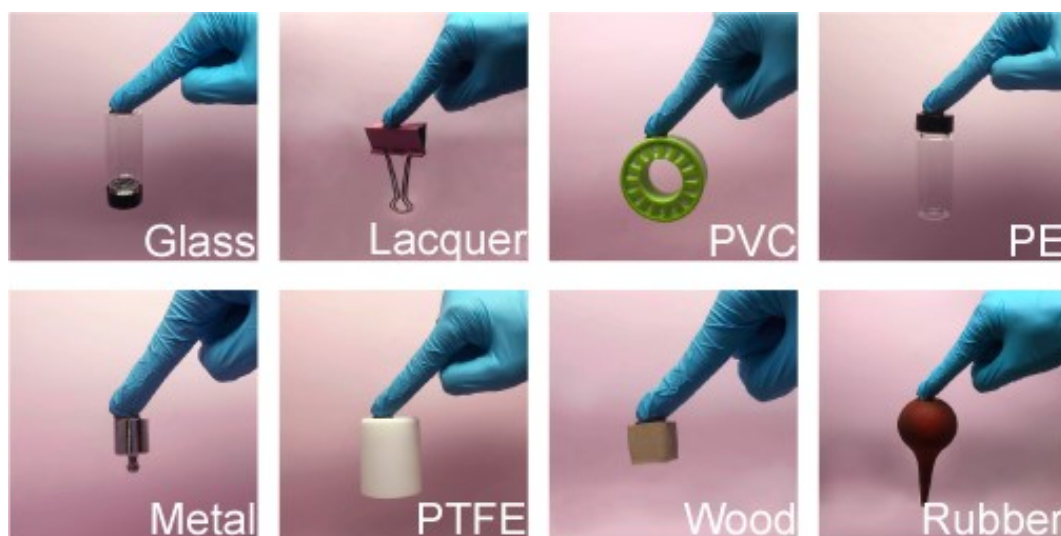**Fig. S7.** ^{1}H-NMR hydrogen spectrum of ADNICs.

Fig. S8. Digital photograph of ADNIC-0.5 adhering to different substrate surfaces.
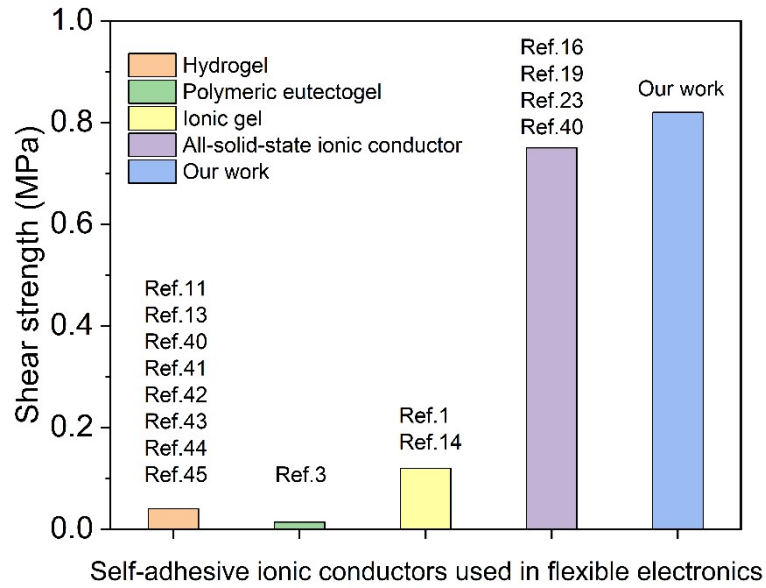
Fig. S9.A comparison between our work and recently reported self-adhesive ionic conductors used in flexible electronics.
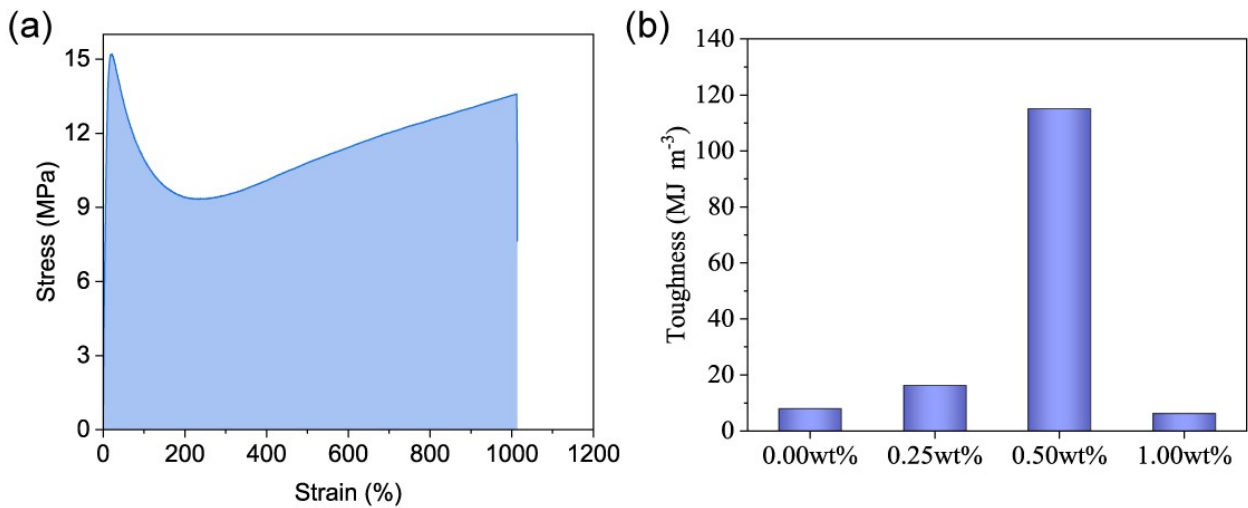

Fig. S10. (a)The tough of ADNICs containing 0.5 wt.% lignin networks. (b)Toughness of ADNICs with different lignin network contents.
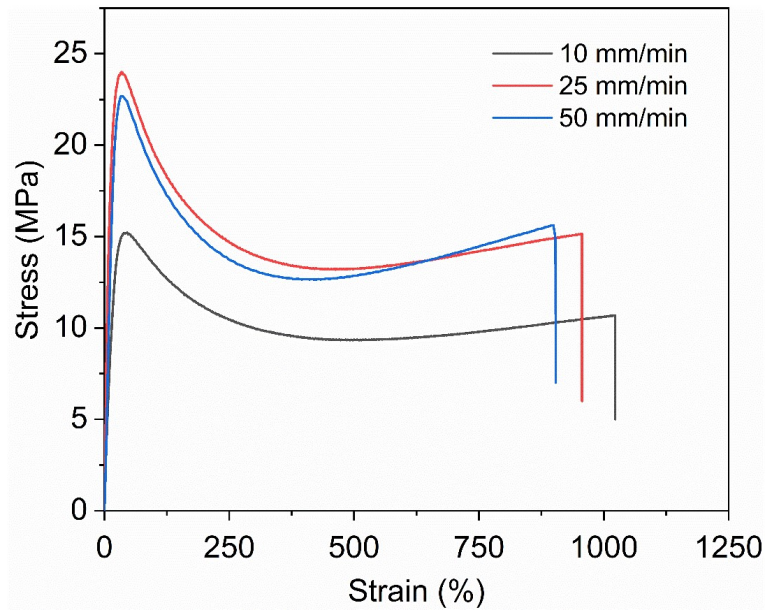
Fig. S11. Stress-strain curves of ADNIC-0.5 at different tensile speeds.
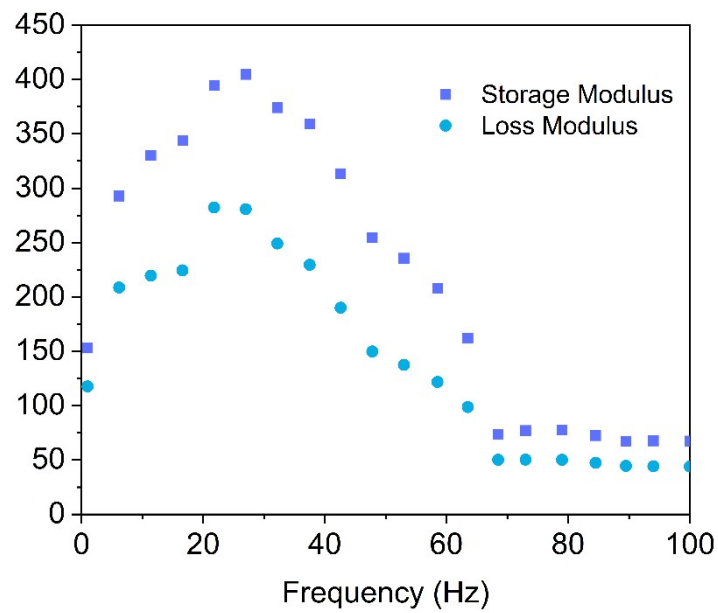

Fig. S12. Storage modulus and loss modulus as functions of frequency for ADNIC-0.5. (The energy storage modulus of ADNIC-0.5 is consistently greater than the loss modulus in the frequency range of 1-100 HZ at room temperature (25°C), indicating the formation of strong crosslinks in the polymer network.)
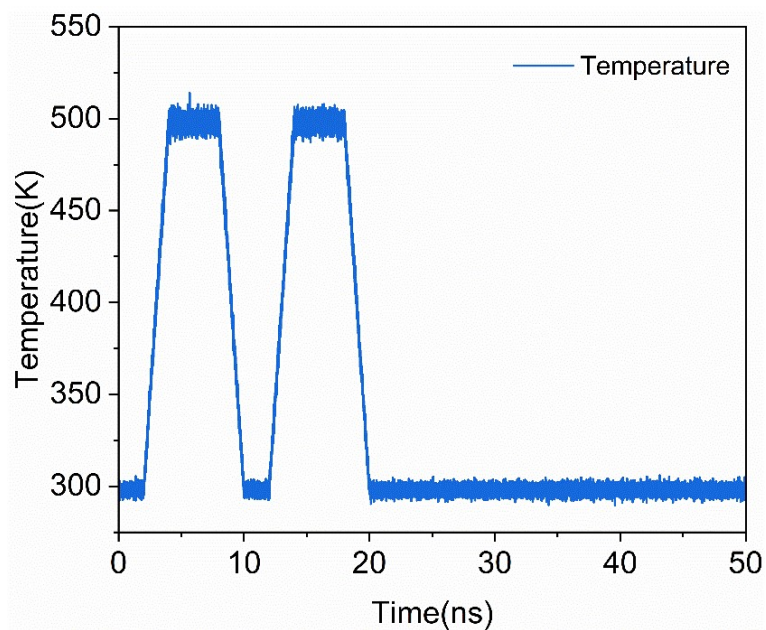
Fig. S13.MD simulations after two temperature ramp-up-cool-down annealing.

Table S2. The average hydrogen bonding interaction energy of lignin with each component in the last 5 ns.

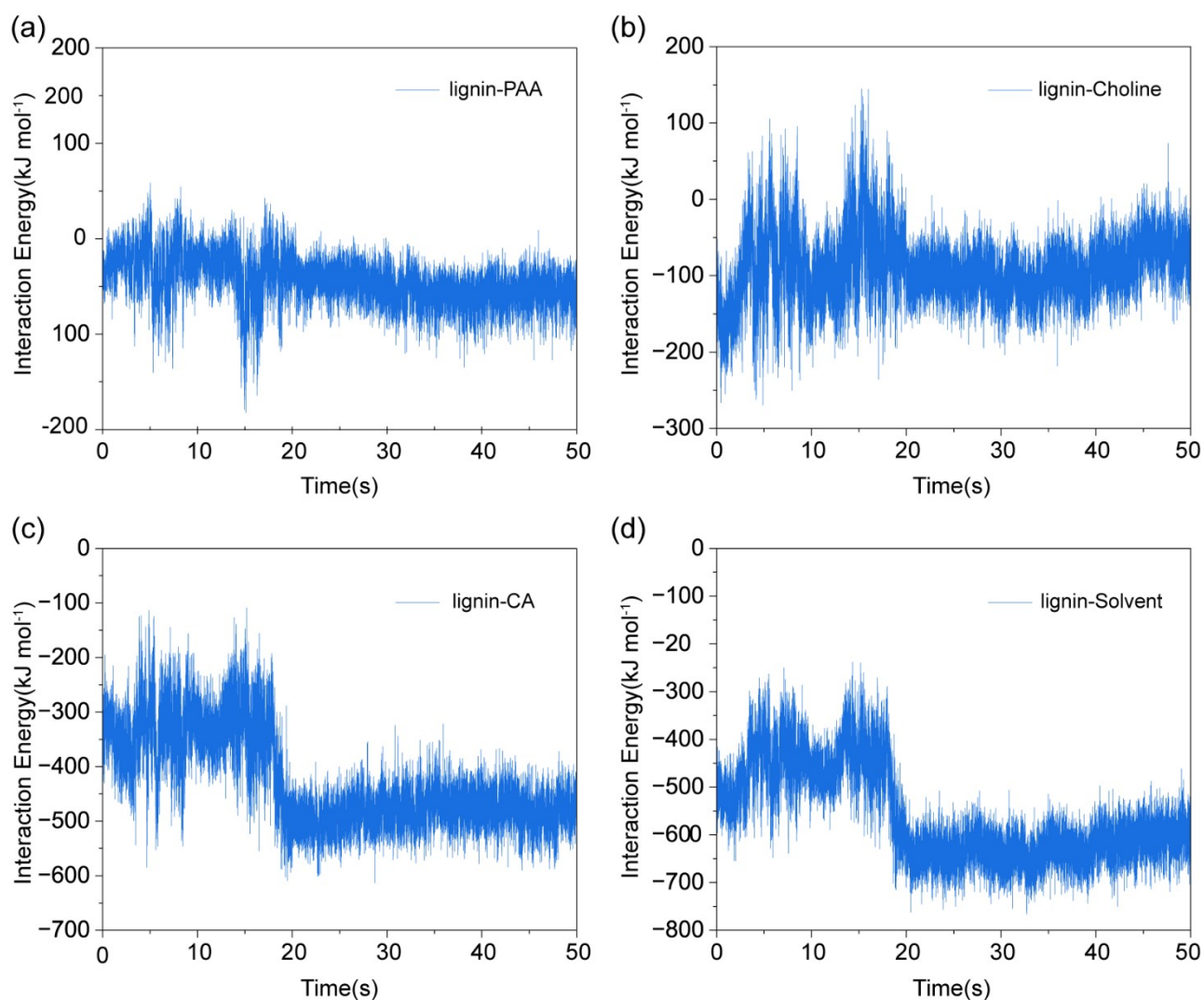| lignin	PAA	Choline	CA	Solvent
Interaction energy(kJ mol^{-1})	-54.37	-63.91	-484.45	-602.74

Fig. S14. Hydrogen bonding interaction energies of lignin with PAA, Choline, CA, and Solvent obtained from MD simulations.

Table S3. Specific locations of hydrogen bonding within ADNICs.

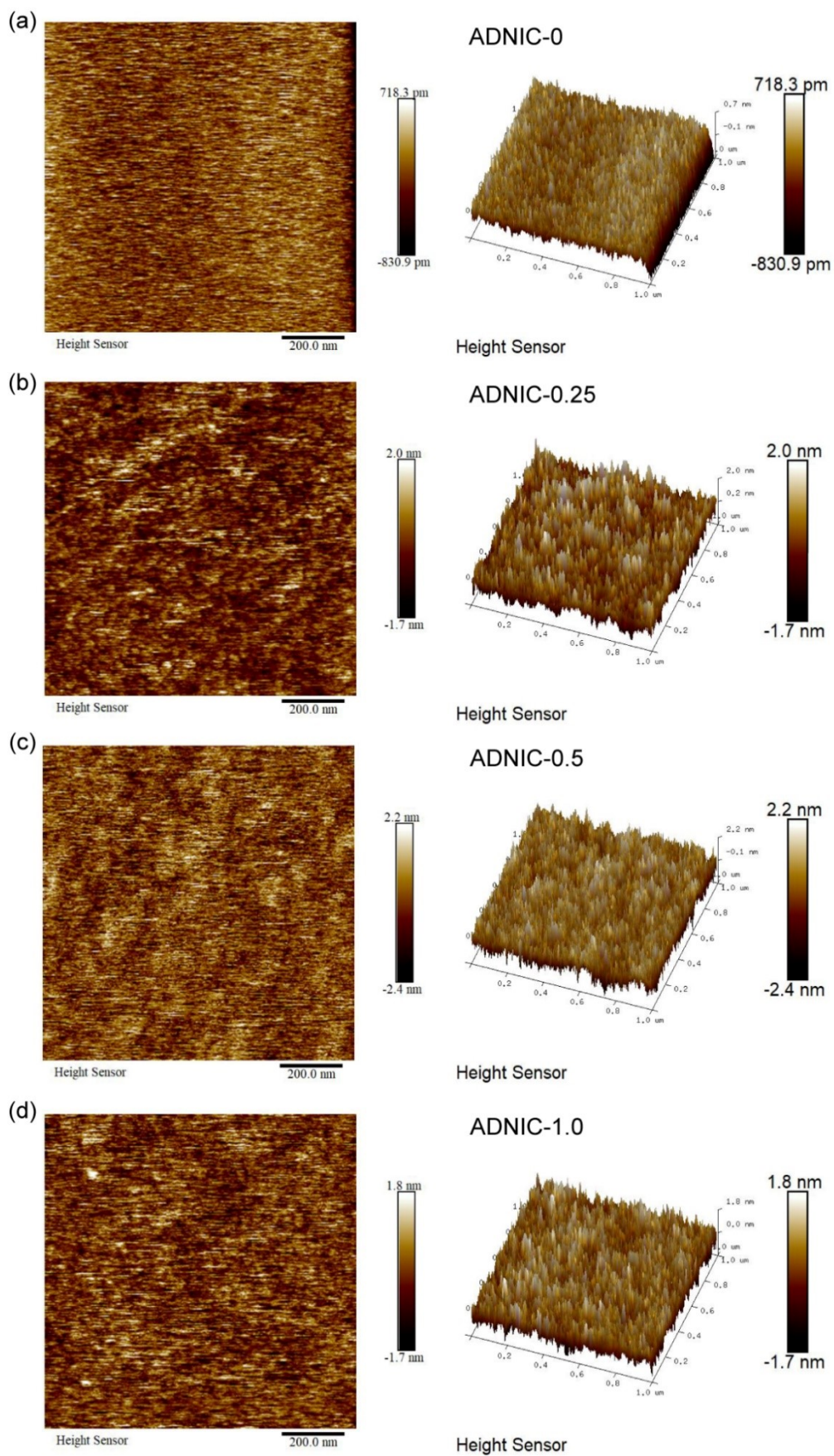| Molecule	Atom	Atom	Molecule	Atom	Atom
Lignin1	O8	H28	PAA796	O6	
	O8		CIA492	O1	H5
	O14	H47	CHO63	O1	
	O1	H1	CIA426	O6	
	O17	H56	CIA490	O7	
	O21		CIA490	O4	H7
	O20	H63	CIA510	O7	
	O25	H80	CIA572	O1	
	O25		PAA774	O1	H4
	O27	H87	CIA491	O2	
	O28	H89	CIA491	O2	

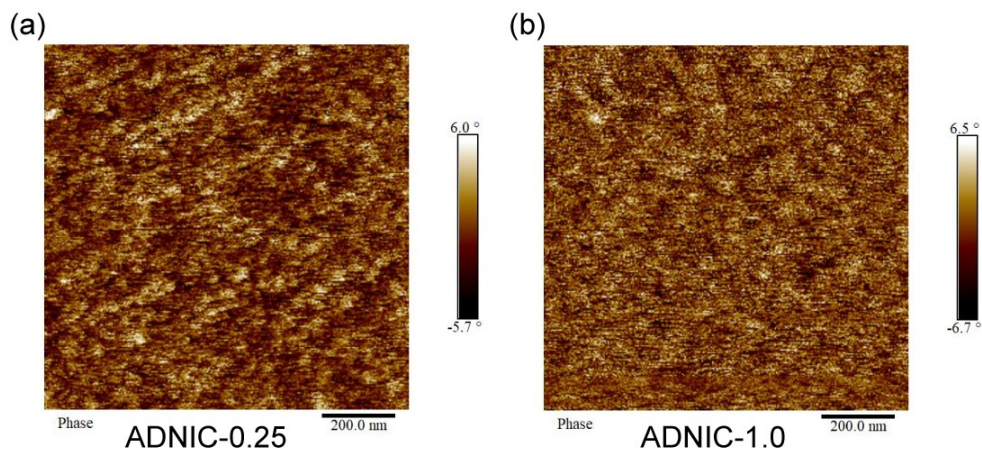**Fig. S15**. The AFM surface morphology and 3D image of ADNICs.

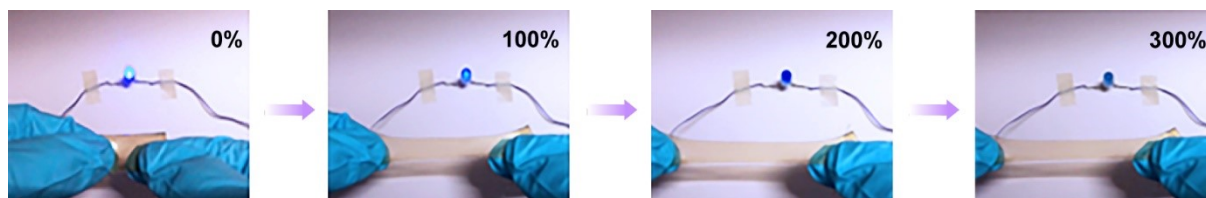**Fig. S16**. The AFM phase diagram of (a) ADNIC-0.25 and (b)ADNIC-1.0.

Fig. S17. Optical images of ADNIC-0.5 sensors at 0%, 100%, 200%, and 300% tensile strain.

Table S4. Comparison of our work with the recently investigated performance comparison of all-solid-state ionic conductors.

Material name	Adhesion strength(glass)	Tensile strength (MPa)	Strain at break(%)	Toughness	Transparency	Conductivity	Self-healing	Reference
Ionic conductive elastomers (ICEs)	No	1.05-7.1MPa	~1744%	3897-221752 J m^{-2}	Yes	Yes	Yes	2
Ion-conducting fluorinated elastomer (ICFE)	No	770 kPa	>6000%	17.1 MJ m^{-3}	Yes	Yes	Yes	4
Solvent-free ionic conductive elastomers (ICEs)	No	~300 KPa	997 %	□	Yes	Yes	Yes	10
Ionic triboelectric nanogenerator (iTENG)	Yes	340 kPa	1036%	□	Yes	Yes	No	15

Solid-state PIL-based copolymers	25 kPa	0.24 ± 0.02 MPa	540 ±50%	0.64 ± 0.02 MJ m^{-3}	No	Yes	Yes	16
Bioderived polymerizable deep eutectic solvent ionic elastomers	No	5.39 MPa	~100%	4.87 MJ m^{-3}	No	Yes	Yes	17
Hydropho-bic deep eutectic polymers (HDEPs)	100 N m^{-1}	~22 kPa	~175%	□	No	No	Yes	19
POSS–TMB–LiMTFSI ionic conductor	143 kPa	0.37 MPa	88.96%	□	Yes	Yes	Yes	20
Dry ion-conducting dynamic bottlebrush networks (DICDBNs)	38 kPa	99 kPa	923%	□	Yes	Yes	Yes	21
Ionic conducting elastomers (ICEs)	~100 N m^{-1}	~0.24 MPa	~1100%	□	Yes	Yes	No	23
Poly(AAm/ChCl-co-MA/ChCl) elastomers	No	~0.34 MPa	450%	□	Yes	Yes	Yes	24
Poly(AA/ChCl-co-MA/ChCl) elastomers	No	~0.03 MPa	1450%	□	Yes	Yes	Yes	25
Poly(PDES)-PA elastomers	No	~0.43 MPa	1300%	□	Yes	Yes	Yes	26
Stiff, self-healable, transparent polymer (SSHTP)	No	65.74 ~ 108.13 MPa	2.03%-9.06%	□	Yes	Yes	Yes	27
Conductive elastomers (CEs)	No	31.21 MPa	3645%	615 MJ m^{-3}	Yes	Yes	Yes	28

Liquid-free double network ionic conductors (LFDNICs)	No	71.3 MPa	671%	268 MJ m^{-3}	Yes	Yes	Yes	29
Lithium salt elastomers (LSEs)	~500N m^{-1}	46.7-214KPa	350 %-400%	11.01-65.88 MJ m^{-3}	Yes	Yes	Yes	30
Self-adhesive liquid-free double-network ionic conductors (SALFDNICs)	757 N m^{-1}	0.58 MPa	1200%	1.4 MJ m^{-3}	Yes	Yes	Yes	31
Self-adhesive dry ionic conductor (SADIC)	~3.5MPa （4500N m^{-1}）	17.90-0.03 MPa	400%-4600%	□	Yes	Yes	Yes	40
All-solid-state double-network ionic conductors (ADNICs)	~5500 N m^{-1}	13.59 MPa	~1013%	115.042MJ m^{-3}	Yes	Yes	Yes	Our work

References:

1. A. H. M. Case D A, Belfon K, et al, University of California, San Francisco, 2021.
2. J. M. Wang, W. Wang, P. A. Kollman and D. A. Case, *J. Mol. Graph.*, 2006, 25, 247-260.
3. J. M. Wang, R. M. Wolf, J. W. Caldwell, P. A. Kollman and D. A. Case, *J. Comput. Chem.*, 2004, 25, 1157-1174.
4. T. Lu and F. W. Chen, *J. Comput. Chem.*, 2012, 33, 580-592.
5. M. J. Abraham, T. Murtola, R. Schulz, S. Pall, J. C. Smith, B. Hess and E. Lindahl, *SoftwareX (Netherlands)*, 2015, 1-2, 19-25.
6. L. Martinez, R. Andrade, E. G. Birgin and J. M. Martinez, *J. Comput. Chem.*, 2009, 30, 2157-2164.
7. H. J. C. Berendsen, J. P. M. Postma, W. F. van Gunsteren, A. DiNola and J. R. Haak, *J. Chem. Phys. (USA)*, 1984, 81, 3684-3690.
8. G. Bussi, D. Donadio and M. Parrinello, *J. Chem. Phys. (USA)*, 2007, 126, 7.
9. E. F. Pettersen, T. D. Goddard, C. R. C. Huang, E. E. C. Meng, G. S. Couch, T. I. Croll, J. H. Morris and T. E. Ferrin, *Protein Sci.*, 2021, 30, 70-82.